A Kinetic Approach to Synergize Bactericidal Efficacy and Biocompatibility in Silver-Based Sol-Gel Coatings

Thibaut Zwingelstein[1], Agathe Figarol[1], Vincent Luzet[1], Maude Crenna[2], Xavier Bulliard[2], Alba Finelli[2], Julien Gay[2], Xavier Lefèvre[2], Raphaël Pugin[2], Jean-François Laithier[3], Frédéric Chérioux[1], Vincent Humblot[1*].*

AUTHOR ADDRESS

1 : Université Franche-Comté, CNRS, FEMTO-ST, F-25000 Besançon, France.

2 : Centre Suisse d'Electronique et de Microtechnique CSEM SA, Jaquet Droz, 1 CH-2000 Neuchâtel, Switzerland.

3 : Coloral SA, Chemin des Devins 28, 2088 Cressier, Switzerland

KEYWORDS silver, bactericidal material, bactericide, cytotoxicity, biocompatibility, kinetics, sol-gel.

ABSTRACT

Silver ions are antimicrobial agents with a powerful action against bacteria. Applications in surface treatments, as Ag^+ functionalized sol-gel coatings, are expected in the biomedical field to prevent contaminations and infections. The potential cytotoxicity of Ag^+ cations towards human cells is well-known though. However, scarce are the studies that consider both the bactericidal activity and the biocompatibility of the Ag^+ functionalized sol-gels. Here, we demonstrate that the

cytotoxicity of Ag^+ cations is circumvented thanks to the ability of Ag^+ cations to kill *Escherichia coli (E. coli)* much faster than normal human dermal fibroblasts (NHDF). This phenomenon was investigated in the case of two silver nitrate-loaded sol-gel coatings: one with 0.5 w/w% of Ag^+ cations and the second with 2.5 w/w%. The maximal amount of released Ag^+ ions overtime (0.25 mg/L) was ten times lower than the minimal inhibition (MIC) and minimal bactericidal (MBC) concentrations (respectively 2.5 mg/L and 16 mg/L) for *E. coli*, and twice lower to the minimal cytotoxic concentration (0.5 mg/L) observed in NHDF. *E. coli* were killed 8 to 18 times, respectively, faster than NHDF by silver loaded sol-gel coatings. This original approach, based on the kinetic control of the biological activity of Ag^+ cations instead of a concentration effect, ensures the bactericidal protection, while maintaining the biocompatibility of the Ag^+ cations functionalized sol-gels. This opens promising applications of silver loaded sol-gel coatings for biomedical tools in short-term or indirect contacts with the skin.

I. INTRODUCTION

Ag^+ ions and Ag-based compounds have been used for centuries as antimicrobial agents towards a large spectrum of bacteria, viruses and even fungi, with different efficacies as a function of the targeted microorganism [1] over different forms such as colloid, suspension, powder or gel [2]. Different materials can be chosen as a host matrix to stabilize Ag-based compounds as a surface coating: polymers, ceramics, or hybrid organic-inorganic materials. In the last category, coatings based on sol-gel chemistry are particularly interesting due to the wide range of microstructures that can be generated through the choice and ratio of precursors, and of the drying and curing conditions. In particularly, the density and porosity of the coating can be tuned, and the sol-gel materials can act as a reservoir of silver-based compounds, with a controlled release depending on its porosity[3].

For conferring antimicrobial activity to sol-gel coatings, different approaches and different Ag^+ sources can be used. A first method consists in mixing the sol-gel solution with a silver salt ($AgNO_3$) before coating the mix on the desired surface. In a second approach, the silver salt can be reduced to form finely dispersed Ag^0 colloids either before or after coating on the surface, by dipping the coating in reducing solution. In a third approach, silver Ag^0 nanoparticles can be directly mixed with the sol-gel solution before coating the surface. In the cases of nanoparticles or colloids, the drawbacks are the rapid change of sol-gel coatings properties, such as a drastic modification of the color and transparency, or an alteration in the mechanical or protective properties with low amounts of colloids or particles present at the surface of the coatings. The incorporation of $AgNO_3$ salt, on the other hand, barely modifies the initial properties of the coatings. The release of Ag^+ cations to the surface, should however be properly controlled for bacteria contact killing. The kinetics of release through the sol-gel has not been quantified yet and is one of the topics of this study. Furthermore, the possible cytotoxic effect on human cells with regards to the bactericidal effect is still controversial.

The role of silver as an antimicrobial agent has been widely studied, however its impacts on mammal and human cells should indeed be further addressed. This is a fairly common issue among the research against drug-resistance bacteria. The same physicochemical properties that give metal nanoparticles an antimicrobial potential [4], can lead to worrying toxic impact on the human health [5–7]. Based on a literature review, only a few scientific articles considered both points when studying silver-loaded sol-gel coatings (see Supplementary Information) [8–12]. In a review published by Simchi *et al.* [8] it was stated that in given concentrations, silver was not toxic for human cells. The authors were referring to 3 articles to support this argument: the first one [13] did not contain any

results on biocompatibility; in the second one [14] no difference in cytotoxicity between hydroxyapatite coating with or without Ag were observed, however on extracts only and without negative control; finally the third article [15] showed a significant decrease in cells viability after exposition to hydroxyapatite coating containing 0.21-0.45 wt% Ag from $AgNO_3$ mixed with hydroxyapatite and coated on titanium substrates with micro-arc oxidation. The other articles studying both the bactericidal and the cytotoxicity properties of Ag containing sol-gels gave contradictory results with two showing a significant toxicity and two showing no toxicity. Zhang *et al.* [12] used Ag nanoparticles with polytetrafluoroethylene as a sol-gel coating and studied both the impacts on bacteria and mammal cells. They showed that it was efficient against *E. coli* (bacterial biomass accumulation down to 10% after 1 day, and 50% after 7 days). Nevertheless, the authors expressed concerns for local toxicity as they observed a decrease in mouse fibroblasts activity (MTT assay) and morphological observations related to cell stress: loss of their typical spindle-shape, cytoplasmic condensation or shrinkage, and rounded cells. Jaiswal *et al.* [10] studied silver-nitrate and silver-coumarin complex doped sol-gel coatings for their bactericidal effects on *Staphylococcus aureus* and *Enterobacter cloacae*, and cytotoxic impacts on human keratinocytes. Unfortunately, the bactericidal efficiency seemed to be linked with a cytotoxic effect. Rahmani *et al.* [11] assessed a bioactive glass doped with silver oxide: $60SiO_2$-(31-x) $CaO–4P_2O_5–5Li_2O$-xAg_2O, and on the contrary showed no decrease in cell viability on mouse osteoblasts, while exhibiting a bactericidal activity against *E. coli*. Likewise, Aksakal *et al.* [9] observed no decrease in human osteoblast-like cells exposed to glass loaded with selenium and 5 to 20 wt% $AgNO_3$. The differences in the matrix chemistry, cell and bacteria types, and expression of the Ag concentrations hinder the comparisons between the rare studies on the subject.

The literature is more abundant on silver potential cytotoxicity as a free ion form, not embedded in a sol-gel matrix. The present study will focus on mammal and human fibroblasts as a model for dermal and connective tissues. There is a weak consensus on biocompatible doses about 0.5-1 mg/L Ag^+ [16–18]. However, while below 1 mg/L there might be no decrease in fibroblasts viability, other signs of toxicity are present. At 0.45 mg/L a decrease in protein expression and impairs in DNA synthesis can be observed [17]. Between 0.5 and 1 mg/L, a significant increase in the production of reactive oxygen species can be initiated [18].

These findings highlight the crucial importance of a toxicity assessment on human tissues while developing an Ag^+ based bactericidal sol-gel coatings. In this study, we have developed a new strategy to prevent the cytotoxicity of Ag^+ cations while maintaining their bactericidal property. This strong achievement is due to the ability of Ag^+ cations to kill bacteria much faster than human dermal cells. This approach paves the way for applications of silver loaded sol-gel coatings for biomedical materials in short-term or indirect contacts with the skin such as some medical tools and utensils.

The physicochemical properties of two sol-gel coatings containing silver, were first assessed. Their impacts on a model bacterial, *E. coli,* and normal human dermal fibroblasts (NHDF) were investigated with a conventional dose-dependent and an innovative time-dependent approaches. This original perspective, based on a kinetic control of the biological activity of Ag^+ cations instead of a concentration effect, could ensure a bactericidal protection, while maintaining the biocompatibility of the sol-gels.

II. MATERIALS & METHODS

II.1. Chemicals

$AgNO_3$, phosphate buffer saline (PBS), tetraethylorthosilicate, isobutyltrimethoxysilane, nitric acid, ethanol, isopropanol, Ciprofloxacin, Ampicillin, Chloramphenicol, Streptomycin, Penicillin, Triton X-100, microbiological agar and Luria Bertani broth, bovin gelatin, cell medium (DMEM, 2% glutamine), trypsin-EDTA (0.25%-0.02%), trypan blue, and fetal bovine serum were purchased from Merck, Fisher, Gelest and TCI Chemicals and used without any further treatment.

II.2. Sol-gel

Sol gel formulation:

The base sol-gel formulation was composed of tetraethylorthosilicate (TEOS, 17.8 mL), isobutyltrimethoxysilane (3.6 mL), ethanol as a solvent (10.7 mL), and acidified water (2% vol. HNO_3; 9.4 mL) as catalyst. A 100 mL beaker was placed in cold water bath, as the sol-gel hydrolysis reaction is exothermic. Isobutyltrimethoxysilane, with a saturated bond, was added to slightly decrease the sol-gel network density and avoid cracking of the sol-gel layer. The components were added successively, with the acidified water at last, dropwise. Powdered silver nitrate (0.5 or 2.5 wt% in Ag) was then added to the solution under continuous stirring. Stirring was pursued during 30 min to ensure a perfect dissolution. The solution turned slightly gray.

Sample coating:

Glass slides (microscope glass, DWK Life Science) were used as substrate. Before sol-gel deposition, the slides were cleaned in isopropyl alcohol during 10 min under sonication. Deposition was carried out by dip coating using a KSV Nima Medium (Biolin Scientific, Finland). The glass slides were dipped into the sol-gel solution for a few seconds and removed at a constant speed of 100 mm/min. A scheme of the sol-gel coating route is represented schematically in Scheme 1. After coating, the slides were allowed to dry for 10 min. The coated slides were then placed into an oven, pre-heated at 60°C, for curing. The temperature was then raised to 100°C for 1 hour, and cooled again to 60°C before removing after 1 additional hour. The glass slides were then cut into pieces of 0.5 cm x 0.5 cm by laser cutting for further tests. The thickness of the coating was measured using a stylus profilometer (Burker Dektak XT) and reached 0.61 µm for a sol-gel without $AgNO_3$, and respectively 0.65 µm and 0.69 µm for a sol-gel with 0.5 and 2.5 wt% of Ag. The morphology of the sol-gel coatings has been investigated by scanning electron microscopy (**Figure S1**). No significant changes in deposit morphology were observed based on the amount of silver content in the sol-gel.

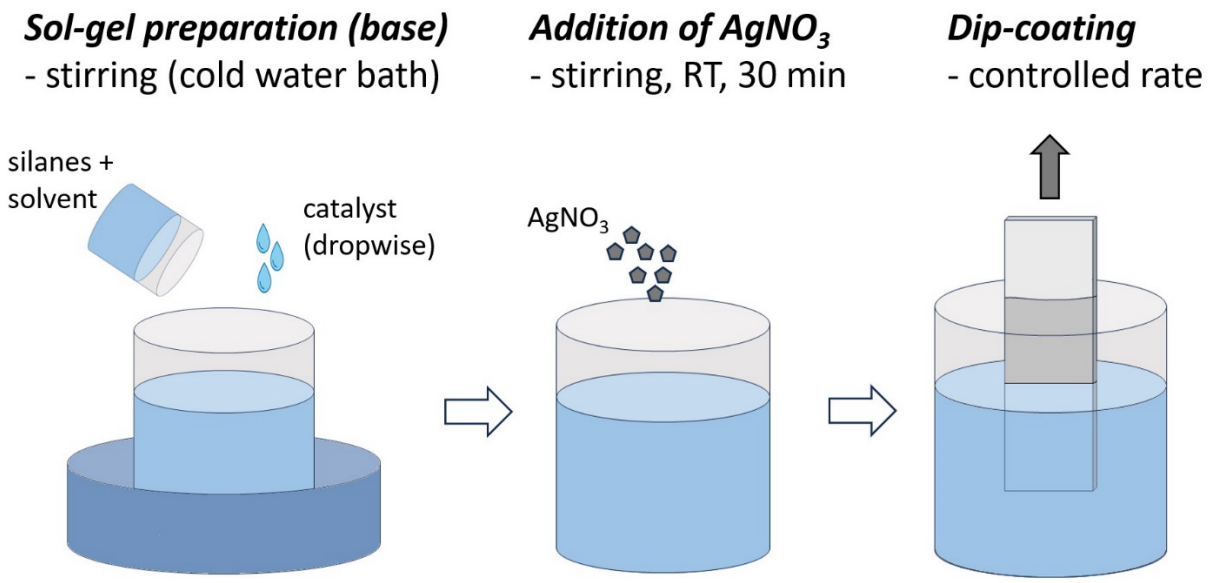

Scheme 1: Scheme of samples preparation for sol-gel coating consisting of a preparation of the base sol-gel solution, the addition of AgNO3 in the form of powder, and the dip coating process on glass slides.

The chosen $AgNO_3$ concentration range (0.5 and 2.5 wt%) was set, for the lower limit, to guaranty sufficient release from the coating (as explained below) and for the upper limit, to form a homogeneous coating on the glass. Above this limit, the coating gradually got an unwanted grey color.

II.3. Preparation of $AgNO_3$ solutions.

$AgNO_3$ solutions for microbiology experiments were freshly prepared in Milli-Q water at initial Ag^+ concentration of 800 mg/L and diluted as needed for the different *in vitro* experiments.

II.4. ICP-AES experiments

II.4.1. Release experiments.

Glass slides loaded with sol-gel, sol-gel 0.5 and 2.5 % Ag^+ cations were suspended in 5 mL PBS at 30 °C and stirred at 90 rpm. For each indicated time, the whole solution was recovered and replaced by 5 mL of fresh PBS. Ag^+ cations concentrations in solution were determined using Inductively Coupled Plasma Atomic Emission Spectrometry (ICP-AES). Standard control was achieved by analyzing a calibrated solution at 5 mg/L.

II.4.2. Ag^+ cations incorporation within bacteria

2.10^6 CFU/mL of *E. coli* were put in contact in 10 mL of $AgNO_3$ solution in PBS at a concentration of 5 mg/L Ag^+ cations for 30 minutes at 30 °C under 90 RPM agitation. The control solution was 10 mL of PBS with $AgNO_3$ at a concentration of 5 mg/L of Ag^+ cations.

II.5. Bacteria culture

Escherichia coli ATCC 25922 were stocked at -80 °C in glycerol stock. Inoculum were prepared by first growing a solid culture on biological Agar (15 mg/L) + LB (20 mg/L) Petri dished incubated overnight at 30°C. Thus, liquid cultures were carried out by recovering 1 colony from the solid growth Petri dish and inoculated in 5 mL of LB media at 20 mg/L and cultured overnight at 30°C under 90 RPM agitation.

II.5.1. Contact Killing

Exponentially growing *E. coli* in LB was harvested by centrifugation (5000×g, 5 min, 25 °C), washed twice with PBS and suspended in PBS to obtain a concentration of 10^9 CFU/mL. 50 µL of this bacterial suspension were spread onto 89 mm Petri dishes filled with Agar + LB media, using an Interscience EasySpiral automatic seeder. Thus, glass slides were deposited face-down on the

freshly incubated Petri dishes by avoiding the creating of air bubbles. After overnight incubation at 30 °C, the photos were recorded using an Interscience Colony Counter Scan 300. Controls were run without loading of $AgNO_3$ in the sol-gel matrix.

II.5.2. Minimal Inhibition Concentration (MIC) and Minimal Bactericidal Concentration (MBC) experiments

MICs values towards *E. coli* were determined using the two-fold dilution method. Experiments were performed in 96-well microplates as triplicate in culture media (LB), with an initial bacterial concentration of approximately 10^6 CFU mL^{-1}. The highest concentrations were prepared according to the following: $AgNO_3$ in distilled water at Ag concentration of 320 and 64 mg/L resulting in concentration in the first well of 80 and 16 mg/L, respectively. After overnight incubation at 30°C, MICs values were determined as the lowest concentration of the compound with no visible bacterial growth. Sterility control (culture broth only), growth control (culture broth with bacteria) and death control (culture broth with bacteria and ethanol:H_2O v/v 70/30) assessed the quality of each experiment.

E. coli MBCs determination was performed by measuring the 96-wells plate in a UV-spectrophotometer the optical density (OD) at 620 nm wavelength, after determination of the MIC values and resuspension of the bacterial pellets. MBC values were determined when the OD value was less than 0.001x the OD of the control growth.

II.5.3. Kinetics of bactericidal action

Exponentially growing *E. coli* in LB was harvested by centrifugation (5000×g, 5 min, 25 °C), washed twice with PBS and suspended in PBS to obtain a concentration of 10^6 CFU/mL. 10 mL of this bacterial suspension were incubated at 30°C under 90 RPM agitation. At each time of the

assay (0-5-10-15-20-25-30-40-50-60-75-90-120-150-180 min), 100 µL of the solution was recovered and diluted 10 and 100 times in PBS. Thus, 50 µL of both dilutions were spread onto 89 mm Petri dishes filled with LB + agar (20 g/L + 15 g/L respectively), using an Interscience EasySpiral automatic seeder. After overnight incubation at 30°C, the CFUs were enumerated were recorded using an Interscience Colony Counter Scan 300. Controls were run without loading of $AgNO_3$ in the bacterial solution.

Ag^+ cations concentrations were chosen as a function of MIC values at MIC/2, and MIC i.e. 1.25, and 2.5 mg/L, respectively.

II.5.4. Evaluation of incorporated Ag in bacteria

10^6 CFU/mL of *E. coli* were put in contact in 10 mL of $AgNO_3$ solution in PBS at a concentration of 5 mg/L Ag^+ cations for 30 minutes at 30°C at 90 RPM agitation. Thus, bacteria were centrifuged and separated from the supernatant, and both resulting solutions were analyzed by ICP-AES to determine Ag^+ cations concentration. 4 solutions were analyzed: a control at 5 mg/L in Ag (S1), the mix bacteria + $AgNO_3$ (S2), and finally a solution with the centrifugated bacteria (S4) vs its supernatant (S3).

II.6. Cell culture

NHDF from abdomen were graciously provided by Dr. Céline Viennet from UMR 1098 RIGHT INSERM EFS UBFC. Cells were culture in Dubelcco's Modified Eagle Medium (DMEM) with 2% glutamine, complemented with 10% fetal bovine serum (FBS), and 1% penicillin-streptomycin (100 U/mL and 0.1 mg/mL respectively), and incubated at 37°C, 5% CO_2 in a humidified

atmosphere. The cells were passaged every 3 or 4 days, and seed at 10 000 cells/cm^2 for culture maintenance.

II.6.1. Cytotoxicity assays

For the assessment of Ag^+ cations toxicity from free $AgNO_3$ powder, 28 000 cells/cm^2 in DMEM without FBS were seeded in 96 well plates (90 000 cells/mL, 100 µL/well). The cells were incubated 24 h for optimum adhesion, then exposed to 0 to 6 mg/L of Ag^+ cations equivalent (addition of 100 µL/well of concentrated $AgNO_3$ solutions). For the assessment of Ag^+ cations toxicity from sol-gel film release, 30 000 cells/cm^2 in DMEM without FBS were seeded in 24 well plates on top of 1 cm^2 sol-gel samples (60 000 cells/mL, 1 mL/well, 1 sample/well, no sample in control wells). For both experiment type, the cells were then incubated for 24 h at 37°C, 5% CO_2 before microscopic observations, and cytotoxicity assays.

The cell viability was evaluated using a MTT assay (3-(4,5-dimethylthiazol-2-yl)-2,5-diphenyltetrazolium bromide). Cells in the positive control well were exposed to 10% v/v Triton X-100 for 30 min. The MTT kit (Merck, reference 11465007001) was used according to the manufacturer's recommendations. Basically, 10% v/v of MTT labelling reagent was added into the cell supernatant, after a 4 h incubation at 37°C, 5% CO_2, 100% v/v of stabilization solution was then added. The absorbance was read at 600 nm after an overnight incubation at 37 °C, 5% CO_2 (Clariostar plate reader, BMG Labtech).

Before the MTT assay, 10 µL of cell supernatants were collected and transferred to a new 96 well plate to assess cell necrosis by measuring LDH (lactate dehydrogenase) release. The LDH kit (Merck, MAK380) was used according to the manufacturer's recommendations. Briefly, 100 µL of LDH mix reagents were added to the 10 µL supernatant. After 30 min incubation at room

temperature, protected from light, 10 µL of stop solution was then added. The absorbance was then read at 450 nm (Clariostar plate reader).

LDH cytotoxicity assay was conducted for $AgNO_3$ free powder. Black 96 well plates with transparent bottoms coated with porcine gelatin (1% m/v) were used for this assay. Cells in the positive control well were exposed to Ethanol 70% v/v for 5 min. The live-dead kit (Merck, CBA415) was used according to the manufacturer's recommendations. After removal of the supernatants, 100 µL of Live-Dead mix was added per well (0.4 µL/mL calcein, 1.7 µL/mL propidium iodide, 0.4 µL/mL Hoechst, in 50% v/v DMEM without FBS, and 50% v/v PBS). After a 30 min incubation at 37°C, 5% CO_2, the fluorescence was read at 490/515 nm, 535/617 nm, et 361/486 nm (Ex/Em, Clariostar plate reader), and pictures were taken with a fluorescent microscope (Axio observer, Zeiss).

II.6.2. Kinetics of the cytotoxicity

The same experimental conditions were used to prepare the cells for the toxicity assay of $AgNO_3$ free powder and for the kinetics assay with only 3 concentrations: 0mg/L, 1.25 mg/Land 2.5 mg/L Ag^+ cations (equivalent to MIC/2 and MIC). For the kinetics assay however, the cells were observed directly after exposure to $AgNO_3$. Pictures were taken with a wide field microscope, at x100 magnification, every 5 min from t0 to t30 min, every 10 min from t30 to t60 min, every 15 min from t60 to t90 min, and every 30 min from t90 to t180 min. Image analyses were carried out by two different experimenters with the ImageJ software, and the cell counter plugin. Cells presenting a healthy morphology (adherent, slender fibroblasts) were counted separately from cells presenting an apoptotic morphology (round, detached, blebbing). Viability results were calculated as the average number of healthy cells divided by the total number of cells (> 60 cells per images, three images per condition, 3 independent experiments).

II.7. Statistical analyses

Three independent experiments were carried out for each assay in triplicates, except when precised. Error bars represent standard deviations. Two by two comparisons of results (sample versus control) were performed. Student's t-test firstly assessed the variance similarity of the two groups. p values were then calculated using two-tailed Fisher test. A difference was considered significant if * $p < 0.05$, or ** $p < 0.01$, or *** $p<0.0005$.

For Figure 1, standards deviations were obtained from measurements carried out on standard solution, ending up to a 1.4 % deviation applied to all ICP-AES data.

RESULTS

Experiments were performed to investigate the potential release of Ag^+ cations bactericidal moieties from the sol-gel films loaded with $AgNO_3$. The results are presented in **Figure 1**, showing ICP-AES measurements of the Ag^+ cations concentration in solution after immersion of Ag^+ loaded sol-gel coated glass slides in PBS solutions. Time-lapse assays were performed successively for 1 hour of immersion, repeated 8 times (from 1 h to 8 h in x-axis), and a further 24 h immersion was performed (32 h in x-axis). For each considered time, the PBS solution was renewed before the next time-slot.

For the 0.5 % Ag^+ loaded sol-gel film, after an initial release close to 0.20 mg/L for the 2 first hours, the release amount dropped to 0.10 mg/L for the next 6 hours-assays. Further 24 h immersion led to an average concentration of 0.15 mg/L. For the 2.5 % Ag^+ loaded film, the measured concentrations were comprised between 0.20 and 0.25 mg/L regardless of the number of successive immersions, and of the length of immersion (1 or 24 h). These results showed, first, that the

films acted as Ag^+ cations reservoirs able to release active product in solution as a function of time. Secondly, one can note that the 0.5 % films start to be depleted after 2 immersions of 1 h. Furthermore, even after 24 h of immersion, the initial concentration of around 0.20 mg/L was not reached anymore confirming the depletion of the matrix, showing that the release was not driven by time or kinetics. Concerning the 2.5% loaded film, the released quantities were stable regardless the numbers of immersion or the duration of the immersion. This result led to the conclusion that an ionic and/or solubility equilibrium was reached upon release of Ag^+ cations in the PBS solution limiting the maximum quantity of Ag^+ cations in solution.

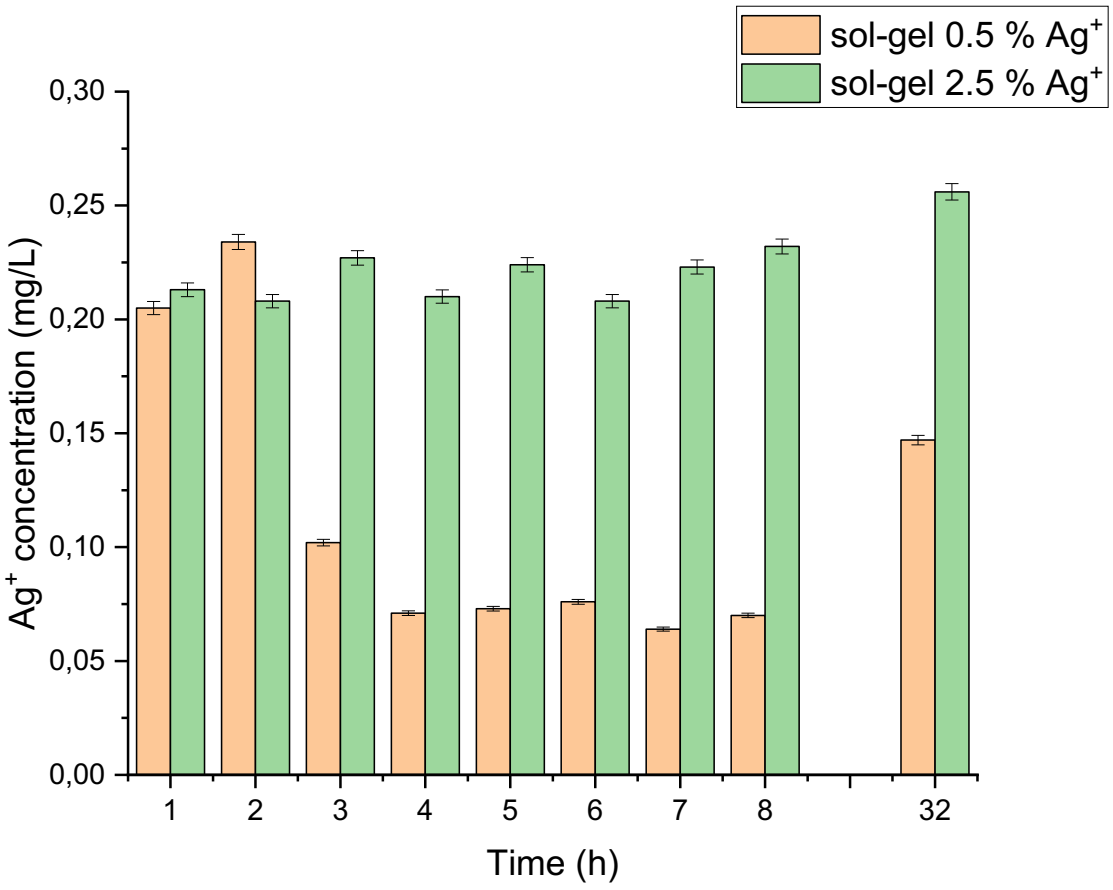

Figure 1: Ag^+ release in PBS at 30°C for sol-gel coatings loaded with 0.5 and 2.5 mass % of Ag.

The present study focused on *E. coli*. Experiments were carried out to determine the Minimal Inhibition Concentration (MIC) that demonstrates the lowest level of antimicrobial agent that inhibits growth, and the Minimal Bactericidal Concentration (MBC) tests that demonstrate the lowest level of antimicrobial agent resulting in microbial death. **Tables S1, S2** and **Figure S2**. presents the MIC/MBC obtained *in vitro* for *E. coli* ATCC 25922 strain. One can see that from these data, MIC and MBC were evaluated at 2.5 mg/L and 16 mg/L, respectively, showing therefore greater antibacterial activities than commonly used antibiotics, thus reinforcing our choice of Ag^+ cations for bactericidal coatings.

The antimicrobial properties of Ag^+ cations may lead to side toxicity for human cells. The cytotoxicity of Ag^+ cations towards NHDF was assessed after 24 h exposures. The results can be found in supplementary data (**Figure S3**). From 0.75 mg/L, a dose-dependent decrease in cell viability, and an increase in cell necrosis was observed. Over 1 mg/L however, the cytotoxicity reached a plateau with less than 40% cells remaining viable, while no, or scarce necrosis was noticed. Microscopic observations confirmed a decrease in the number of live cells after exposure to Ag^+ cations (almost no live cells, stained with calcein, visible above 1.5 mg/L). The live-dead kit uses propidium iodide to label dead cells, which stains only the necrotic cells. Again, scarce stained necrotic cells were observed, while observation before staining showed a morphology typical from apoptotic cells (round, blebbing, and detached). Ag^+ cations seemed thus to induce apoptosis at concentrations higher than 0.75 mg/L. The observed levels of released Ag^+ cations from the sol-gel coating after 24 hours in a row (data named 32h) (**Figure 1**), show maximum concentration of released Ag^+ of 0.25 mg/L, which is half of the lower tested dose (0.5 mg/L, Figure S3A), and therefore should not endangered those human cells within the time frame.

To evaluate the bactericidal efficiency of the sol-gel coatings loaded with $AgNO_3$, contact killing assays were performed on agar Petri dishes previously inoculated with 50 µL of *Escherichia coli* bacteria at 10^6CFU/mL, as show in **Figure 2.A.** Sol-gel films with and without Ag^+ loadings were deposited on the inoculated Petri dished, and after overnight (*eg.* 16 hours) at 30°C the evaluation of the bacterial growth was carried out. The bare sol-gel matrix without $AgNO_3$, **Figure 2.B.** did not show any bactericidal effect as one can notice the presence of bacteria colonies under the glass slide. On the opposite, once the sol-gel matrix was loaded with $AgNO_3$, differences were observed, **Figures 2.C. and D.** First, it can be underlined that under the glass slides, no bacterial colonies were observed, suggesting contact killing or at least inhibition growth of inoculated bacterial upon contact with the $AgNO_3$ sol-gel coatings. Moreover, for the sol-gel films loaded with 2.5% Ag^+ (**Figure 2.D.**), an inhibition growth halo is observable in the areas surrounding the coated glass slides, clearly suggesting a migration of the bactericidal products, *i.e.* Ag^+ compounds, hence suggesting release of the products from the sol-gel films.

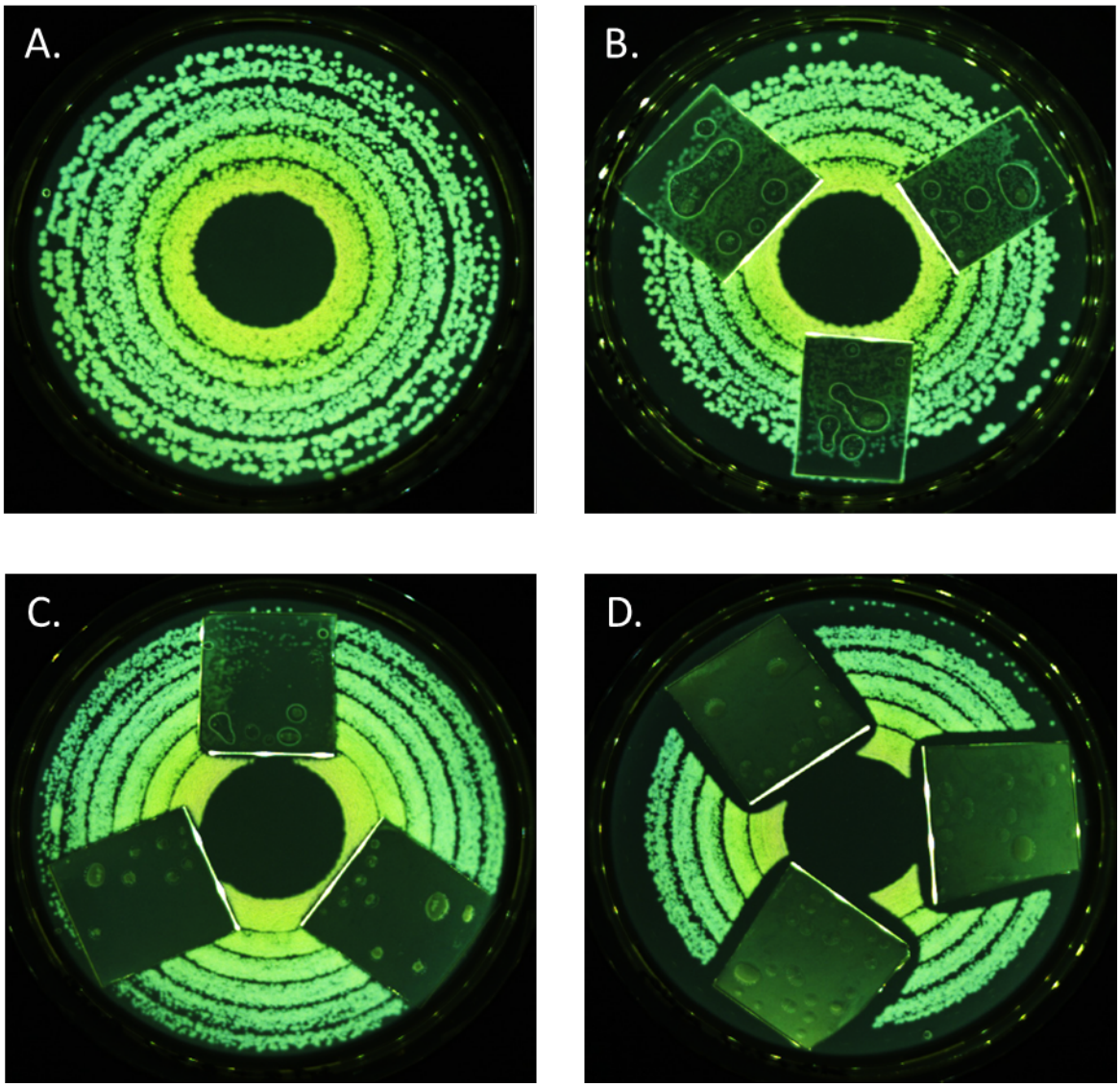

Figure 2: Petri dishes spread with 50 µL of *E. coli* inoculum at 10^9 CFU/mL. A: growth control; B: Sol-gel matrix 0% $AgNO_3$; C: Sol-gel 0.5 % $AgNO_3$; D: Sol-gel 2.5 % $AgNO_3$. % $AgNO_3$ is ex-pressed as mass % of Ag^+ cations within the sol-gel matrix.

However, from those results in **Figure 2**, a release concentration within the range of 0.15 to 0.25 mg/L Ag^+ cations (**Figure 1**) seems to be enough to have an effective bactericidal effect, while *in vitro* MIC/MBC experiments (**Table S1**) highlight the fact that at least a concentration of 2.5 mg/L to 16 mg/L is required to observed the first bactericidal effect towards the same *E. coli* strain. This

factor x10 is quite surprising and could be explained by the method used for the ICP-AES release experiments. In fact, it was suggested that the highest release concentration is obtained once the solubility equilibrium is reached. This suggests that an external factor could either change the solubility value or decrease the Ag^+ concentration within the solution. This last point would end up with the sol-gel reservoir to liberate more Ag^+ in solution to reach again the equilibrium.

In this purpose, we have designed a simple experiment to elucidate the fact that a release concentration of 10 time less than the MIC value was nonetheless able to show a bactericidal effect. Results are presented in **Figure S4**, showing both control solutions S1 and S2 as well as samples solutions S3 and S4. As expected both S1 and S2 solutions had a concentration in Ag^+ cations close to the initial concentration, i.e. 5 mg/L, with respectively 5.040 and 4.900 mg/L. Analyses of the solutions S3 and S4 after separation showed also very interesting results; after 30 minutes, more than 90 % of the Ag^+ cations were present in the bacteria (S4, $C°_{Ag}$=4.510 mg/L) while only 10 % of Ag^+ cations remained in the supernatant (S3, $C°_{Ag}$=0.478 mg/L), with the addition of S3 + S4 (4.988 mg/L) being almost equal to the initial concentration of 5 mg/L.

Based on this experiment, it seems clear that upon contact for 30 minutes between *E. coli* and $AgNO_3$ solution, 90 % of the Ag^+ cations were incorporated with the bacteria, therefore depleting the concentration of free Ag^+ in solution resulting in the ionic and/or solubility equilibrium to be disturbed. Keeping in mind this conclusion, this means that for the contact killing experiments presented in **Figure 2**, and performed during 16 hours, after release of the initial 0.15 to 0.25 mg/L of Ag^+ cations, the rapid incorporation of Ag^+ cations within *E. coli* bacteria enables the sol-gel reservoir to release more Ag^+ cations in the solution, up to potentially reach concentration values close to the *in vitro* MIC/MBC values, thus explaining the bactericidal effect and inhibition halo observed for both sol-gel loaded with 0.5 and 2.5 % of Ag^+ cations.

Concomitantly, this meant that even if the measured released concentrations of Ag^+ cations from the sol-gel film were under the limit of cytotoxicity in mammal cells (**Figures 1 and 3**), the potential incorporation of Ag^+ cations within the cells could enhance more releasing from the sol-gel reservoir, thus decreasing the expected biocompatibility. Assays were carried out to assess fibroblasts response after a 24 h growth on the sol-gel surfaces. The cells displayed changes in morphology after exposure to the sol-gels (**Figure 3.A.**). The bare sol-gel induced a reduced cell growth, with some round shape fibroblasts, signs of a moderate cytotoxicity. Once loaded with 0.5 or 2.5% Ag^+, the sol-gel seemed to impair the cell adhesion, or to lead to a strong cytotoxicity as all cells were rounded, blebbing and for most of them, detached from the surface. The quantitative viability assay (potency for mitochondrial reduction of MTT) is in line with these observations (**Figure 3.B.**). The bare sol-gel was responsible for a slight decrease in viability to 78 ± 13. which remains over the 70% considered as standard viability expectation [19]. Ag^+ cations contained in the loaded sol-gel induced however a significant decrease in viability, down to 17 ± 17% and 23 ± 10% for 0.5% and 2.5% Ag^+ respectively. To check whether this effect was due to a possible release of silicon present in the coating, ICP-AES analyses were carried out following the same parameters as for Ag^+ cations, this time focusing on silica leaching. The results showed a limited release of silica over time (between 0.05 and 0.2 ppm), attesting to the stability of the sol-gel layer. By changing either the curing conditions or the sol-gel composition to form a denser sol-gel network, this release can be suppressed (or below the limit of detection). The results of the LDH assay can be found in supporting information (**Figure S5**). As for the assessment of the free $AgNO_3$ powder, the Ag^+ loaded into the sol-gel did not seem to lead to necrosis, but rather apoptosis. Regarding those three result groups, the hypothesis of the sol-gel acting as a reservoir seemed to be confirmed.

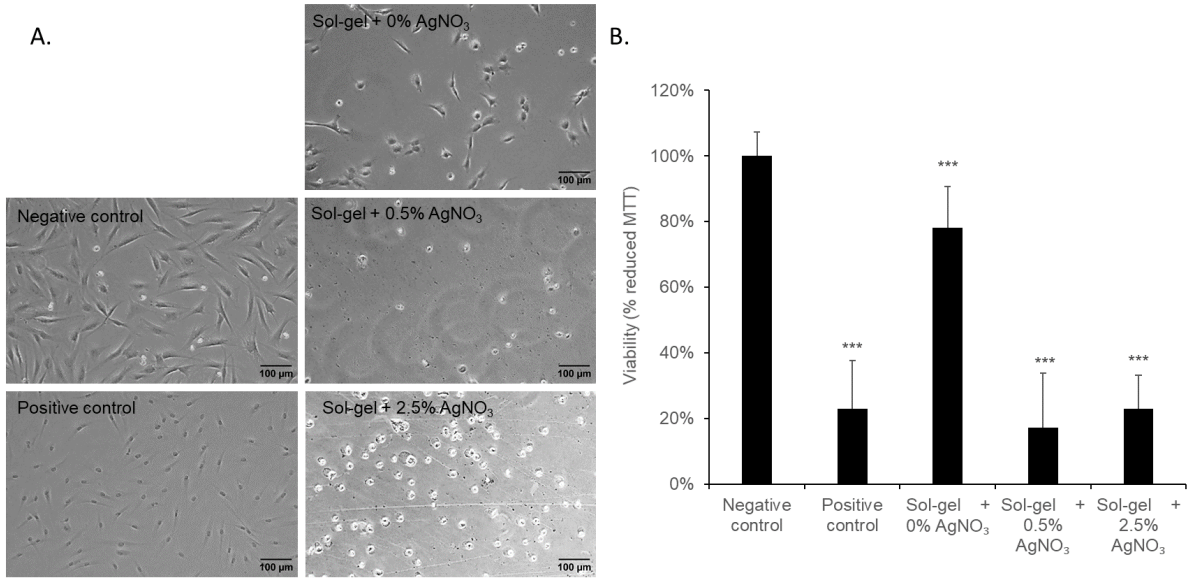

Figure 3 : Cytotoxicity of the sol-gel films loaded with 0.5% or 2.5% $AgNO_3$ (i.e. 0.5 % wt or 2.5 % wt of Ag^+). A: Microscopic observations of the fibroblasts after a 24 h growth on the sol-gel films, or in a culture well without (negative control) or with 10% Triton X-100 (positive control). B: Fibroblasts viability after 24 h, expressed as percentages of reduced MTT salt compared with the negative control (*** $p<0.0005$).

This set of experiments has demonstrated the difficulty to find a thermodynamic range for which the Ag^+ cations bactericidal protection would be achieved, while maintaining the biocompatibility of the sol-gel. Could however a kinetic range be possible? The bacteria and cells were once again exposed to Ag^+ cations at the MIC and MIC/2 (2.5 and 1.25 mg/L, respectively) (**Figure 4**, and microscopy observations in **Figure S6**). As expected, the bacteria viability dropped significantly in a very short time, while the cell response kinetics was slower. A decrease to 70% of viability was observed after 20.6 min for cells and 2.7 min for bacteria exposed to 2.5 mg/L Ag^+ cations (**Figure 4.A.**); or after 23.6 min for cells and 3.1 min for bacteria exposed to 1.25 mg/L Ag^+ cations

(**Figure 4.B.**). The sol-gel loaded with Ag^+ cations could thus lead to a bactericidal effect 8 to 18 times faster than a toxic response towards mammal cells.

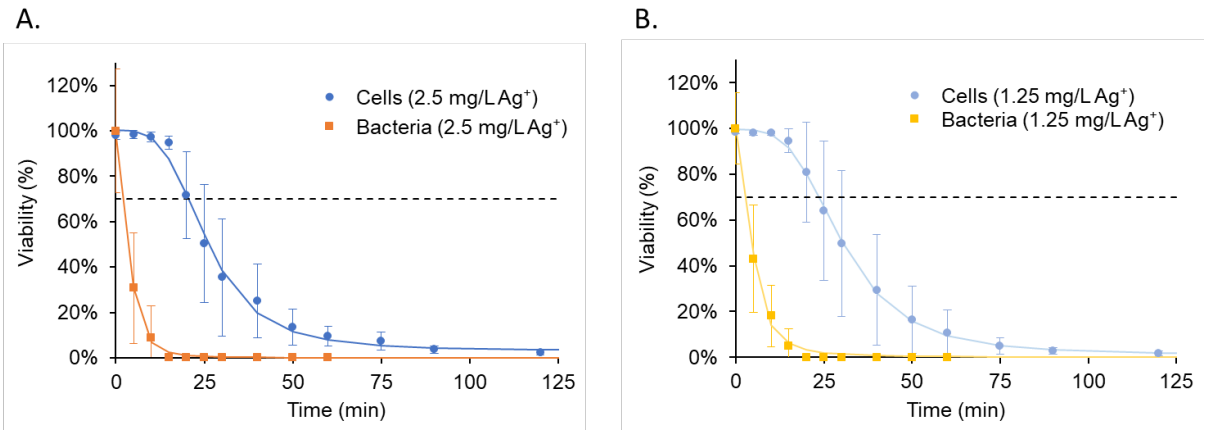

Figure 4: Kinetic of the viability decrease after exposure of cells (blue dots) or bacteria (yellow squares) to 2.5 mg/L (A.) or 1.25 mg/L (B.) Ag^+ cations from $AgNO_3$ (corresponding to the MIC and MIC/2). Three independent experiments in triplicates were carried out for the cell kinetics, two in triplicates for the bacteria kinetics.

III. DISCUSSION

It is widely acknowledged that materials, such as sol-gel materials containing silver (as metal or cations), demonstrate antibacterial properties. Furthermore, chemically durable materials that release Ag^+ cations gradually over an extended period of time are sought after for medical applications. In comparison to the use of standard antibiotics, Ag^+ cations have shown significant bactericidal efficacy without the potential development of antibiotic resistance.

Although the mechanism of the bactericidal action of Ag-based compounds or Ag^+ cations remains unclear, a few hypotheses have emerged in the recent literature. A common consensus suggests that exposure to Ag^+ cations disrupts the bacterial membrane, leading to the leakage of cytoplasm

and intracellular contents.[2,20] This membrane disruption is often attributed to the strong interactions of Ag^+ cations with the constituents of bacterial membranes, primarily through interactions with thiol groups of membrane enzymes or proteins.[21]

Here, the concentrations at which free Ag^+ cations from $AgNO_3$ impact fibroblast viability (over 0.75 mg/L) align with the literature consensus presented in the introduction.[16–18] These concentrations vary depending on experimental conditions, such as the chosen serum percentage in the medium. In our experiments, a serum-free medium was used, potentially overestimating the toxicity. However, the literature indicates deleterious cell responses at lower exposure doses, particularly at higher serum concentrations.[17]

Furthermore, minimum inhibitory concentration (MIC) and minimum bactericidal concentration (MBC) doses for bacteria were at least three times higher than the toxic doses observed for fibroblasts. Thus, even in the case of potential overestimation, it appears unlikely to find a concentration where Ag^+ cations inhibit bacterial growth while remaining biocompatible for human cells over a 24-hour period. Direct-contact assays were selected to assess the bactericidal and cytotoxic activity of Ag^+ cations loaded sol-gel surfaces. Although the study of extracts from material releases is accepted by regulations on medical devices' biocompatibility,[22] it can underestimate material toxicity and lead to non-pertinent predictions of surface interactions with human tissues.[23] Similarly, the standard viability limit is set at 70%. While a 30% decrease in viability may already suggest a significant impact *in vivo*, such standard are essential for the standardized biological assessment of a material. As mentioned in the introduction, the release of Ag^+ from loaded sol-gel has been scarcely investigated in the literature [8,24] and comparing one study to another is challenging due to the substantial differences in materials.

In a study by Rahmani *et al.* [11], a release of 0.2 mg/mL Ag^+ cation was observed after one day, increasing to 0.4 mg/L after 7 to 14 days from a sol-gel derived quaternary bioactive glass with composition 60% SiO_2–31% CaO–4% P_2O_5–5% Li_2O (mol%). Another study by Luo *et al.* [15] focused on the release of Ag^+ cation from a borate glass doped with 0.75, 1.0, and 2.0 wt% Ag_2O. The first two materials released up to 1 and 1.3 mg/L Ag^+ cation, respectively, and the third one released up to 2.5 mg/L Ag^+ cation during 48 hours, with a significant decrease observed from 48 hours to one week. These examples underscore that variations in materials impact the release rate, plateau, and reservoir capacity of sol-gel coatings, thereby influencing their bioactivity. In our study, we have illustrated that the developed sol-gel matrix demonstrates a release of Ag^+ cations ranging from 0.15 to 0.25 mg/L. These values are significantly lower than those reported in the literature as mentioned above. This difference can be attributed to the nature of the sol-gel matrix, which is effectively cross-linked due to the precise adjustment of the tetraethylorthosilicate/isobutyltrimethoxysilane ratio as well as the method to provide thin films onto glass slides (refer to the Materials & Methods section for details).

The studied sol-gel surfaces released 0.15 to 0.25 mg/L of Ag^+ cations, so 10 times lower than the MIC for *E. coli*, but showed nonetheless a bactericidal effect. ICP-AES backed up the hypothesis of the sol-gel acting as a reservoir while the Ag^+ cations were internalized by bacteria. A similar mechanism is expected for fibroblasts. The results showed that apoptosis was surely the main cell death pathway after exposure to Ag^+ cations. Apoptotic cores retain membrane integrity and if internalized the Ag^+ cations should be kept from being released into the medium. The same equilibrium displacement could occur as for the bacteria and induce Ag^+ cations releasing from the sol-gel matrix. This finding is, at least partly, supported by the literature. Cell exposition to silver

ions has indeed been reported as a cause of apoptosis [25,26] with an internalization of the Ag^+ cations in lysosome-like vehicles, and bounding to collagen fibers.

Rare are the studies focusing on the kinetics of bacteria and cell killing with silver ions. Most of the assessments on mammal cells are carried out after 24 h, as we firstly did, respecting this standard. Zhan *et al.* [27] have however shown than Ag^+ cations were toxic for fibroblasts as soon as 30 min at 5.4 mg/L. Our results confirmed the considerable speed of the cytotoxicity mechanisms of Ag^+ cations against *E. coli*, 8 to 18 faster than against fibroblasts. Considering this, the competition between bacteria and cells internalization should be in favor of bacteria, and reinforce the time delay between both toxic responses, enabling the use of this surface chemistry for bactericidal applications with short contacts with human skin. As for chemical disinfectants such as hypochlorite or phenolic, long term contact with human tissues should be avoided. However, contrary to these current hospital disinfectants, the coated material itself can act as an antimicrobial agent. There is no need for repeated application of the disinfectants. This could be interesting for objects with frequent, brief or indirect contacts with biological tissues. The silver-loaded sol-gel could be a supplementary tool in the complex strategies for disinfection in healthcare [28].

IV. CONCLUSION

The examined silver-loaded sol-gel coatings consistently released Ag^+ cations at constant concentrations. Despite the release concentrations being below toxic levels for bacteria or human skin cells, both bactericidal action and cytotoxicity were observed with the Ag^+ cations loaded sol-gel coatings. The internalization of Ag^+ cations was confirmed, indicating a shift in equilibrium and a reservoir-like behavior of the functionalized sol-gels, continuously releasing Ag^+ cations that eventually reach toxic levels. No concentration range achieved bactericidal protection while

maintaining biocompatibility of the sol-gel coating. Instead, a time range was identified. Due to the time lag between bactericidal and apoptotic actions, with *E. coli* exhibiting a killing time 8 to 18 times faster than fibroblasts, it becomes feasible to consider applications of silver-loaded sol-gel surfaces to significantly reduce the risk of infections and contaminations. While not suitable for implants, these coatings could be beneficial for materials with short-term or indirect skin contact, such as gloves. Surgical tools, doorknobs, or other items in high-risk areas like operating rooms and hospital facilities could benefit from this type of bactericidal coating.

SUPPORTING INFORMATION

The following files are available free of charge: supporting data and figures (as a PDF): extensive literature review; MIC/MBC determinations; microscopy and UV-visible determination of cytotoxicity towards NHDF; ICP-AES data**;** LHD and MTT assays; kinetics microscopic observation of cytotoxicity towards NHDF.

AUTHOR INFORMATION

Corresponding Author

Agathe Figarol: agathe.figarol@femto-st.fr

Vincent Humblot: vincent.humblot@femto-st.fr

Author Contributions

Conceptualization: AFig, XB, RP, JFL, FC, VH. Methodology: AFig, XB, FC, VH. Formal analyses: TZ, AFig, XB, FC, VH. Investigation: TZ, VL, MC, AFin, XL. Supervision: AFig, RP, FC, VH. The manuscript was written through contributions of all authors. All authors have given approval to the final version of the manuscript.

Funding Sources

The authors would like to thank the European cross-border cooperation program Interreg Franco-Suisse 2014–2020 and the FEDER agency (Fonds Européen de Développement Régional) for funding.

ACKNOWLEDGMENT

The authors would like to thank Sylvaine Linget from Laboratoire QUALIO Analyses & Environnement for her help in the Ag release ICP-AES experiments with and without bacteria and Lorine Vacelet from Coloral SA for Si release ICP-AES experiments. The authors would also like to thanks Adeline Marguier and Fanny Lotthammer (FEMTO-ST) for preliminary experiments. This work was partly supported by the French RENATECH network and its FEMTO-ST technological facility.

REFERENCES

(1) Klasen, H. J. Historical Review of the Use of Silver in the Treatment of Burns. I. Early Uses. *Burns J. Int. Soc. Burn Inj.* **2000**, *26* (2), 117–130. https://doi.org/10.1016/s0305-4179(99)00108-4.
(2) Kędziora, A.; Wieczorek, R.; Speruda, M.; Matolínová, I.; Goszczyński, T. M.; Litwin, I.; Matolín, V.; Bugla-Płoskońska, G. Comparison of Antibacterial Mode of Action of Silver Ions

and Silver Nanoformulations With Different Physico-Chemical Properties: Experimental and Computational Studies. *Front. Microbiol.* **2021**, *12*.
(3) Singh, R.; Rento, C.; Son, V.; Turner, S.; Smith, J. A. Optimization of Silver Ion Release from Silver-Ceramic Porous Media for Household Level Water Purification. *Water* **2019**, *11* (4), 816. https://doi.org/10.3390/w11040816.
(4) Mishra, A.; Pradhan, D.; Halder, J.; Biswasroy, P.; Rai, V. K.; Dubey, D.; Kar, B.; Ghosh, G.; Rath, G. Metal Nanoparticles against Multi-Drug-Resistance Bacteria. *J. Inorg. Biochem.* **2022**, *237*, 111938. https://doi.org/10.1016/j.jinorgbio.2022.111938.
(5) Ding, L.; Liu, Z.; Aggrey, M. O.; Li, C.; Chen, J.; Tong, L. Nanotoxicity: The Toxicity Research Progress of Metal and Metal- Containing Nanoparticles. *Mini-Rev. Med. Chem.* **2015**, *15* (7), 529–542.
(6) Sengul, A. B.; Asmatulu, E. Toxicity of Metal and Metal Oxide Nanoparticles: A Review. *Environ. Chem. Lett.* **2020**, *18* (5), 1659–1683. https://doi.org/10.1007/s10311-020-01033-6.
(7) Bakhsheshi-Rad, H. R.; Ismail, A. F.; Aziz, M.; Akbari, M.; Hadisi, Z.; Khoshnava, S. M.; Pagan, E.; Chen, X. Co-Incorporation of Graphene Oxide/Silver Nanoparticle into Poly-L-Lactic Acid Fibrous: A Route toward the Development of Cytocompatible and Antibacterial Coating Layer on Magnesium Implants. *Mater. Sci. Eng. C* **2020**, *111*, 110812. https://doi.org/10.1016/j.msec.2020.110812.
(8) Simchi, A.; Tamjid, E.; Pishbin, F.; Boccaccini, A. R. Recent Progress in Inorganic and Composite Coatings with Bactericidal Capability for Orthopaedic Applications. *Nanomedicine Nanotechnol. Biol. Med.* **2011**, *7* (1), 22–39. https://doi.org/10.1016/j.nano.2010.10.005.
(9) Aksakal, B.; Demirel, M. In Vitro Study of Antimicrobial and Cell Viability on Newly Synthesized Bioglass-Based Bone Grafts: Effects of Selenium and Silver Additions. *Proc. Inst. Mech. Eng. [H]* **2018**, *232*, 095441191879796. https://doi.org/10.1177/0954411918797968.
(10) Jaiswal, S.; Bhattacharya, K.; Sullivan, M.; Walsh, M.; Creaven, B. S.; Laffir, F.; Duffy, B.; McHale, P. Non-Cytotoxic Antibacterial Silver–Coumarin Complex Doped Sol–Gel Coatings. *Colloids Surf. B Biointerfaces* **2013**, *102*, 412–419. https://doi.org/10.1016/j.colsurfb.2012.07.047.
(11) Rahmani, M.; Moghanian, A.; Yazdi, M. S. The Effect of Ag Substitution on Physicochemical and Biological Properties of Sol-Gel Derived 60%SiO2–31%CaO–4%P2O5–5%Li2O (Mol%) Quaternary Bioactive Glass. *Ceram. Int.* **2021**, *47* (11), 15985–15994. https://doi.org/10.1016/j.ceramint.2021.02.173.
(12) Zhang, S.; Liang, X.; Gadd, G. M.; Zhao, Q. A Sol–Gel Based Silver Nanoparticle/Polytetrafluorethylene (AgNP/PTFE) Coating with Enhanced Antibacterial and Anti-Corrosive Properties. *Appl. Surf. Sci.* **2021**, *535*, 147675. https://doi.org/10.1016/j.apsusc.2020.147675.
(13) Rojas, I. A.; Slunt, J. B.; Grainger, D. W. Polyurethane Coatings Release Bioactive Antibodies to Reduce Bacterial Adhesion. *J. Controlled Release* **2000**, *63* (1), 175–189. https://doi.org/10.1016/S0168-3659(99)00195-9.
(14) Chen, W.; Liu, Y.; Courtney, H. S.; Bettenga, M.; Agrawal, C. M.; Bumgardner, J. D.; Ong, J. L. In Vitro Anti-Bacterial and Biological Properties of Magnetron Co-Sputtered Silver-Containing Hydroxyapatite Coating. *Biomaterials* **2006**, *27* (32), 5512–5517. https://doi.org/10.1016/j.biomaterials.2006.07.003.
(15) Song, W.-H.; Ryu, H. S.; Hong, S.-H. Antibacterial Properties of Ag (or Pt)-Containing Calcium Phosphate Coatings Formed by Micro-Arc Oxidation. *J. Biomed. Mater. Res. A* **2009**, *88A* (1), 246–254. https://doi.org/10.1002/jbm.a.31877.

(16) Galandáková, A.; Franková, J.; Ambrožová, N.; Habartová, K.; Pivodová, V.; Zálešák, B.; Šafářová, K.; Smékalová, M.; Ulrichová, J. Effects of Silver Nanoparticles on Human Dermal Fibroblasts and Epidermal Keratinocytes. *Hum. Exp. Toxicol.* **2016**, *35* (9), 946–957. https://doi.org/10.1177/0960327115611969.
(17) Hidalgo, E.; Domínguez, C. Study of Cytotoxicity Mechanisms of Silver Nitrate in Human Dermal Fibroblasts. *Toxicol. Lett.* **1998**, *98* (3), 169–179. https://doi.org/10.1016/S0378-4274(98)00114-3.
(18) Cortese-Krott, M. M.; Münchow, M.; Pirev, E.; Heβner, F.; Bozkurt, A.; Uciechowski, P.; Pallua, N.; Kröncke, K.-D.; Suschek, C. V. Silver Ions Induce Oxidative Stress and Intracellular Zinc Release in Human Skin Fibroblasts. *Free Radic. Biol. Med.* **2009**, *47* (11), 1570–1577. https://doi.org/10.1016/j.freeradbiomed.2009.08.023.
(19) 14:00-17:00. *ISO 10993-5:2009*. ISO. https://www.iso.org/standard/36406.html (accessed 2024-03-04).
(20) Gaudillat, Q.; Krupp, A.; Zwingelstein, T.; Humblot, V.; Strohmann, C.; Jourdain, I.; Knorr, M.; Viau, L. Silver-Based Coordination Polymers Assembled by Dithioether Ligands: Potential Antibacterial Materials despite Received Ideas. *Dalton Trans.* **2023**. https://doi.org/10.1039/D3DT00683B.
(21) Ishida, T. Antibacterial Mechanism of Ag+ Ions for Bacteriolyses of Bacterial Cell Walls via Peptidoglycan Autolysins, and DNA Damages. *MOJ Toxicol.* **2018**, *4*. https://doi.org/10.15406/mojt.2018.04.00125.
(22) International Organization for Standardization. *ISO - 11.100.20 - Biological Evaluation of Medical Devices*; Standard ISO 10993; 2022. https://www.iso.org/ics/11.100.20/x/ (accessed 2023-04-18).
(23) Sussman, E. M.; Casey, B. J.; Dutta, D.; Dair, B. J. Different Cytotoxicity Responses to Antimicrobial Nanosilver Coatings When Comparing Extract-Based and Direct-Contact Assays. *J. Appl. Toxicol.* **2015**, *35* (6), 631–639. https://doi.org/10.1002/jat.3104.
(24) Kawashita, M.; Tsuneyama, S.; Miyaji, F.; Kokubo, T.; Kozuka, H.; Yamamoto, K. Antibacterial Silver-Containing Silica Glass Prepared by Sol-Gel Method. *Biomaterials* **2000**, *21* (4), 393–398. https://doi.org/10.1016/s0142-9612(99)00201-x.
(25) Kaplan, A.; Akalin Ciftci, G.; Kutlu, H. M. The Apoptotic and Genomic Studies on A549 Cell Line Induced by Silver Nitrate. *Tumor Biol.* **2017**, *39* (4), 1010428317695033. https://doi.org/10.1177/1010428317695033.
(26) Kristiansen, S.; Ifversen, P.; Danscher, G. Ultrastructural Localization and Chemical Binding of Silver Ions in Human Organotypic Skin Cultures. *Histochem. Cell Biol.* **2008**, *130* (1), 177–184. https://doi.org/10.1007/s00418-008-0415-x.
(27) Zhan, D.; Li, X.; Nepomnyashchii, A. B.; Alpuche-Aviles, M. A.; Fan, F.-R. F.; Bard, A. J. Characterization of Ag+ Toxicity on Living Fibroblast Cells by the Ferrocenemethanol and Oxygen Response with the Scanning Electrochemical Microscope. *J. Electroanal. Chem.* **2013**, *688*, 61–68. https://doi.org/10.1016/j.jelechem.2012.07.008.
(28) Exner, M.; Bhattacharya, S.; Gebel, J.; Goroncy-Bermes, P.; Hartemann, P.; Heeg, P.; Ilschner, C.; Kramer, A.; Ling, M. L.; Merkens, W.; Oltmanns, P.; Pitten, F.; Rotter, M.; Schmithausen, R. M.; Sonntag, H.-G.; Steinhauer, K.; Trautmann, M. Chemical Disinfection in Healthcare Settings: Critical Aspects for the Development of Global Strategies. *GMS Hyg. Infect. Control* **2020**, *15*. https://doi.org/10.3205/dgkh000371.